Micromachined Devices for Wireless Communications

CLARK T.-C. NGUYEN, MEMBER, IEEE, LINDA P. B. KATEHI, FELLOW, IEEE, AND GABRIEL M. REBEIZ, FELLOW, IEEE

Invited Paper

An overview of recent progress in the research and development of micromachined devices for use in wireless communication subsystems is presented. Among the specific devices described are tunable micromachined capacitors, integrated high-Q inductors, micromachined low-loss microwave and millimeter-wave filters, low-loss micromechanical switches, microscale vibrating mechanical resonators with Q's in the tens of thousands, and miniature antennas for millimeter-wave applications. Specific applications are reviewed for each of these components with emphasis on methods for miniaturization and performance enhancement of existing and future wireless transceivers.

Keywords— *Acoustic resonators, antennas, filters, high-Q, IF, MEMS, micromachining, oscillators, phase noise, resonators, RF, switches, synthesizers, thin-film inductors, transceivers, tunable, wireless.*

I. INTRODUCTION

Vibrating mechanical tank components, such as crystal and surface-acoustic wave (SAW) resonators, are widely used for frequency selection in communication subsystems because of their high quality factor (Q's in the tens of thousands) and exceptional stability against thermal variations and aging. In particular, the majority of heterodyning communication transceivers rely heavily upon the high Q of SAW and bulk-acoustic mechanical resonators to achieve adequate frequency selection in their radio-frequency (RF) and intermediate-frequency (IF) filtering stages and to realize the required low phase noise and stability in their local oscillators. Ceramic (dielectric) resonators or waveguide components are also required at RF or microwave/millimeter-wave frequencies to provide the needed high-Q functions. In addition, discrete inductors and variable capacitors are used to properly tune and couple the front-end sense and power amplifiers. At present, the aforementioned resonators and discrete elements are off-chip components and so must interface with integrated electronics at the board level, often consuming a sizable portion of the total subsystem area. In this respect, these devices pose an important bottleneck against the ultimate miniaturization and portability of wireless transceivers. For this reason, many research efforts have been focused upon strategies for either miniaturizing these components [1]–[5] or eliminating the need for them altogether [6]–[8].

The rapid growth of integrated circuit (IC)-compatible micromachining technologies that yield microscale, high-Q tank components may now bring the first of the above strategies closer to reality. Specifically, the high-Q RF and IF filters, oscillators, and couplers, currently implemented via off-chip resonators and discrete passives, may now potentially be realized on the microscale using micromachined equivalents based on a variety of novel devices, including high-Q on-chip mechanical resonators [9]–[11], voltage-tunable on-chip capacitors [12], isolated low-loss inductors [13]–[16], [34], microwave/millimeter-wave high-Q filters [35]–[40], structures for high-frequency isolation packaging [43], [44], and low-loss micromechanical switches [45]–[50]. Once these miniaturized filters and oscillators become available, the fundamental bases upon which communications systems are developed may also evolve, giving rise to new system architectures with possible power- and bandwidth-efficiency advantages. For systems operating past X-band, antennas can also be micromachined with potential cost savings and with additional capabilities attained via active antenna arrays (e.g., phased arrays, power combining, etc.) [51], [53]–[57].

This paper reviews recent progress in the research and development of microelectromechanical devices for use in communication subsystems. It begins with a brief introduction into the needs of wireless communication transceivers, identifying specific functions that could greatly

Manuscript received January 5, 1998; revised February 27, 1998. This work was supported in part by the Defense Advanced Research Projects Agency, National Science Foundation, National Aeronautics and Space Administration, Army Research Office, Office of Naval Research, and numerous industrial sponsors.

The authors are with the Department of Electrical Engineering and Computer Science, University of Michigan, Ann Arbor, MI 48109-2122 USA.

Publisher Item Identifier S 0018-9219(98)05098-1.

0018–9219/98$10.00 © 1998 IEEE

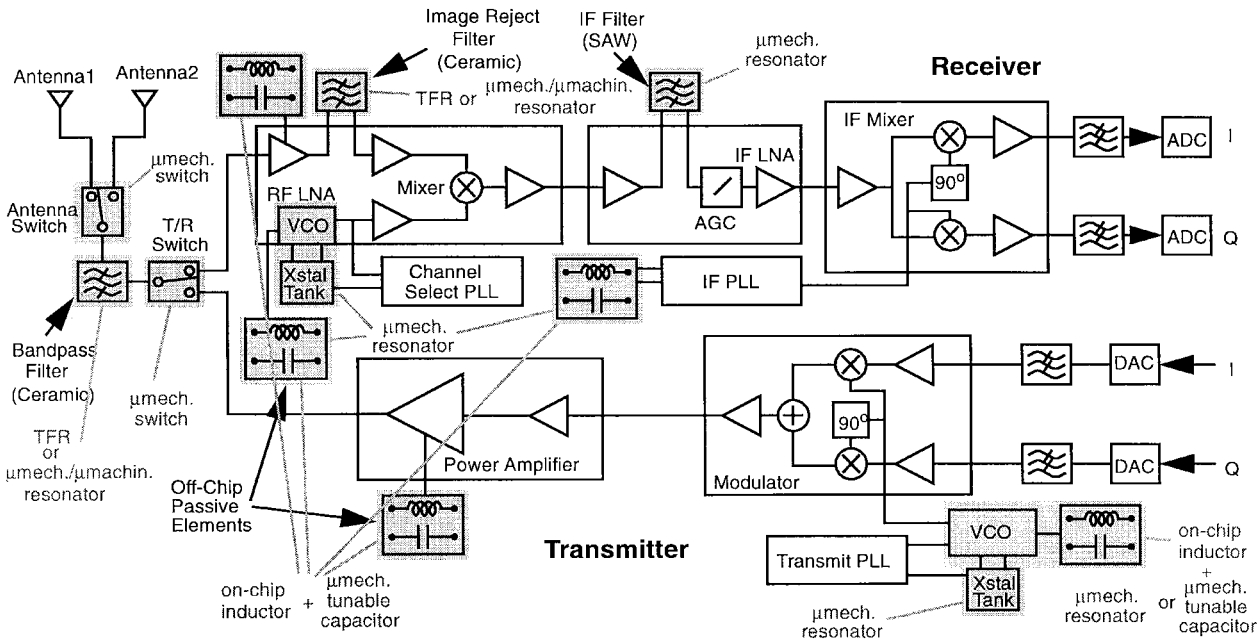

Fig. 1. System-level schematic detailing the front-end design for a typical wireless transceiver. The off-chip, high-Q, passive components targeted for replacement via micromechanical versions (suggestions in lighter ink) are indicated by shading in the figure.

benefit from micromechanical implementation. Several specific devices will then be described, with particular emphasis on frequency-selective microelectromechanical systems (MEMS) for high-Q oscillators and filters. This paper concludes by considering the impact that the discussed devices may have on future transceiver architectures.

II. Miniaturization of Transceivers

To illustrate more concretely the specific transceiver functions that benefit from micromechanical implementation, Fig. 1 presents the system-level schematic for a typical superheterodyne wireless transceiver. As implied in the figure, several of the constituent components can already be miniaturized using integrated circuit transistor technologies. These include the low noise amplifiers (LNA's) in the receive path, the solid-state power amplifier (SSPA) in the transmit path, synthesizer phase-locked loop (PLL) electronics, mixers, and lower frequency digital circuits for baseband signal demodulation. Due to noise, power, and frequency considerations, the SSPA (and sometimes the LNA's) are often implemented using compound semiconductor technologies (i.e., GaAs). Thus, they often occupy their own chips, separate from the other mentioned transistor-based components, which are normally realized using silicon-based bipolar and complementary metal–oxide–semiconductor (CMOS) technologies. However, given the rate of improvement of silicon technologies (silicon-germanium included [17]), it is not implausible that all of the above functions could be integrated onto a single chip in the foreseeable future.

Unfortunately, placing all of the above functions onto a single chip does very little to decrease the overall superheterodyne transceiver size, which is dominated not by transistor-based components but by the numerous passive components indicated in Fig. 1. The presence of so many frequency-selective passive components is easily justified when considering that communications systems designed to service large numbers of users require numerous communication channels, which in many implementations (e.g., time division multiple access) must have small bandwidths and must be separable by transceiver devices used by the system. The requirement for small channel bandwidths results in a requirement for extremely selective filtering devices for channel selection and extremely stable (noise-free) local oscillators for frequency translation. For the vast majority of cellular and cordless standards, the required selectivity and stability can only be achieved using high-Q components, such as discrete inductors, discrete tunable capacitors (i.e., varactors), and SAW and quartz crystal resonators, all of which interface with IC components at the board level. The needed performance cannot be achieved using conventional IC technologies because such technologies lack the required Q. It is for this reason that virtually all commercially available cellular or cordless phones contain numerous passive, SAW, and crystal components.

A. The Need for High Q in Oscillators

For any communications application, the stability of the oscillator signals used for frequency translation, synchronization, or sampling is of utmost importance. Oscillator frequencies must be stable against variations in temperature, against aging, and against any phenomena, such as noise or microphonics, that cause instantaneous fluctuations in phase and frequency. The single most important parameter that dictates oscillator stability is the Q of the frequency-setting tank (or of the effective tank for the case of ring

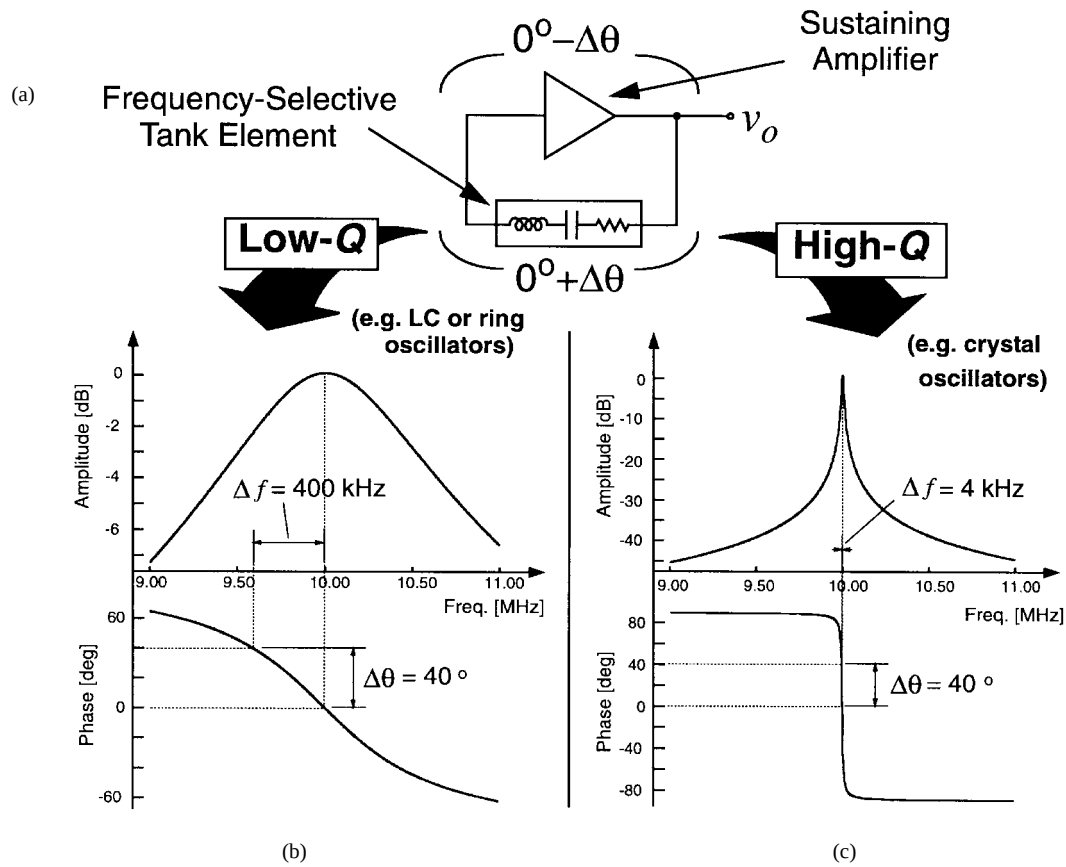

Fig. 2. (a) A simple series resonant oscillator schematic. (b) Bode plot for a low-Q tank, indicating the Δf for a given $\Delta\theta$. (c) Similar to (b) but for a high-Q tank.

oscillators). For a given application, and assuming a finite power budget, adequate long- and short-term stability of the oscillation frequency is insured only when the tank Q exceeds a certain threshold value.

The correlation between tank Q and oscillator stability can be illustrated heuristically by considering the simple oscillator circuit depicted in Fig. 2(a). Here, a series resonant oscillator is shown, comprised of a sustaining amplifier and an inductor-capacitor (LC) tank connected in a positive feedback loop. For proper startup and steady-state operation, the total phase shift around the loop must sum to zero. Thus, if at the oscillation frequency the amplifier operates nominally with a 0° phase shift from its input to its output, then the tank must also have a 0° phase shift across its terminals. Given this, and referring to any one of the tank response spectra shown in Fig. 2(b) or (c), this oscillator is seen to operate nominally at the tank resonance frequency. If, however, an external stimulus (e.g., a noise spike or a temperature fluctuation) generates a phase shift $-\Delta\theta$ across the terminals of the sustaining amplifier, the tank must respond with an equal and opposite phase shift $\Delta\theta$ for sustained oscillation. As dictated by the tank transfer functions of Fig. 2, any tank phase shift must be accompanied by a corresponding operating frequency shift Δf. The magnitude of Δf for a given $\Delta\theta$ is largely dependent on the Q of the resonator tank. Comparison of Fig. 2(b) with (c) clearly shows that a given phase shift incurs a much smaller frequency deviation on the tank with the higher Q. Thus, the higher the tank Q, the more stable the oscillator against phase-shifting phenomena.

To help quantify the above heuristic concepts, one important figure of merit for oscillators is the phase-noise power present at frequencies close to the carrier frequency. Typical phase-noise requirements range from −100 dBc/Hz at 10 kHz deviation from a 1.8 GHz carrier in European Global System for Mobile Telecommunications (GSM) cellular phones to −150 dBc/Hz at 67 kHz carrier deviations in X-band, Doppler-based radar systems [19]. Through a more rigorous analysis of Fig. 1 (assuming linear operation), the phase noise of a given oscillator can be described by the expression [18]

$$\left(\frac{N_{op}}{C}\right)_{f_m} = \frac{FkT}{C}\,\frac{1}{8Q^2}\left(\frac{f_o}{f_m}\right)^2 \text{[dBc/Hz]} \qquad (1)$$

where $(N_{op}/C)_{f_m}$ is the phase-noise power density-to-carrier power ratio at a frequency f_m offset from the carrier frequency, F is the noise figure of the active device evaluated using the total oscillator power P, C is the carrier power delivered to the load, and f_o is the carrier frequency. From (1), phase noise is seen to be inversely proportional to the square of Q and directly proportional to the amplifier noise figure F. Given that F can often be reduced by increasing the operating power P of the sustaining amplifier, (1) then can be interpreted as implying that power and Q can be traded to achieve a given phase-

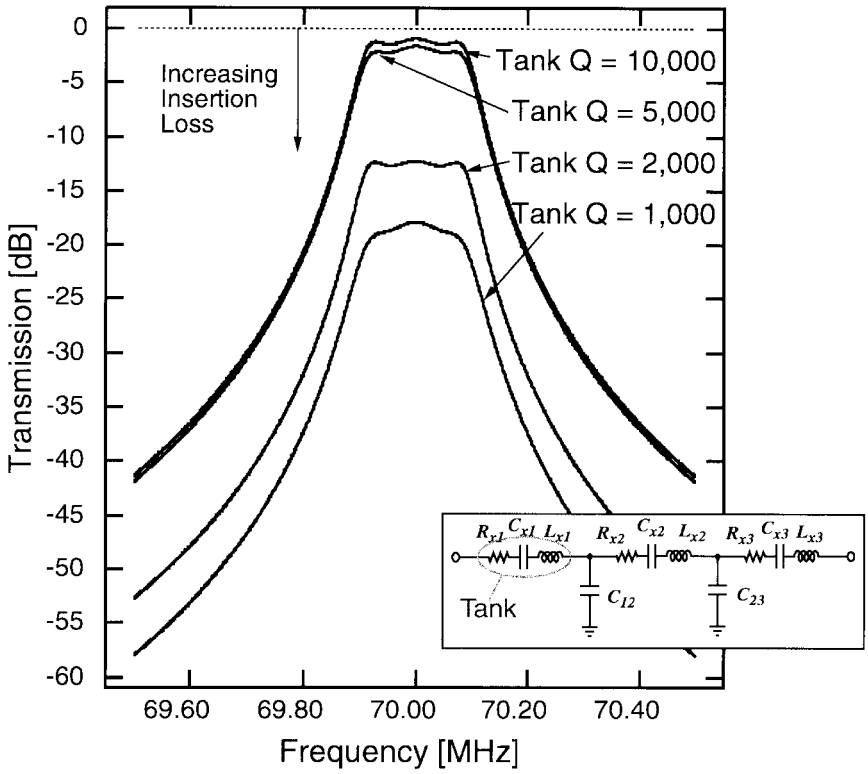

Fig. 3. Simulated frequency characteristics for a 0.3% bandwidth, 70 MHz bandpass filter under varying tank Q's.

noise specification. Given the need for low power in portable units, and given that the synthesizer [containing the reference and voltage-controlled oscillators (VCO's)] is often a dominant contributor to total transceiver power consumption, modern transceivers could benefit greatly from technologies that yield high-Q tank components.

B. The Need for High Q in Filters

Tank Q also greatly influences the ability to implement extremely selective IF and RF filters with small percent bandwidth, small shape factor, and low insertion loss. To illustrate, Fig. 3 presents simulated frequency characteristics under varying resonator tank Q's for a 0.3% bandwidth bandpass filter centered at 70 MHz, realized using the typical LC resonator ladder configuration shown in the insert. As shown, for a resonator tank Q of 10 000, very little insertion loss is observed. However, as tank Q decreases, insertion loss increases very quickly, to the point where a tank Q of 1000 leads to 20 dB of insertion loss—too much even for IF filters and quite unacceptable for RF filters. As with oscillators, high-Q tanks are required for RF and IF filters alike, although more so for the latter, since channel selection is done predominantly at the IF in superheterodyne receivers. In general, the more selective the filter, the higher the resonator Q required to achieve a given level of insertion loss. In particular, the above 0.3% bandwidth filter example applies for IF filters, which, because of their high selectivity, are best implemented with resonator Q's exceeding 5000; RF preselect or image-reject filters, on the other hand, typically require only 3% bandwidths and can thus be implemented using resonators with Q's on the order of 500–1000.

III. Micromechanical Components for Transceivers

As shown in Fig. 1, the front end of a superheterodyne wireless transceiver typically contains a good number of off-chip, high-Q components that are potentially replaceable by micromachined versions. Among the components targeted for replacement in cellular and cordless applications are RF filters, including image rejection filters, with center frequencies ranging from 800 MHz to 2.5 GHz; IF filters, with center frequencies ranging from 455 kHz to 254 MHz; high-Q, tunable, low phase-noise oscillators, with frequency requirements in the 10 MHz–2.5 GHz range; and switches for transmit/receive selection, antenna selection, and multiband configurability. For higher frequency applications (e.g., past X-band), antenna size requirements shrink, so the antenna itself can be manufactured using micromachining techniques. The size of transmission-line filters also shrinks at these frequencies, making them amenable to implementation via micromachining as well.

The following subsections now describe specific microelectromechanical components capable of both miniaturizing and improving the performance of the aforementioned functions.

A. Voltage-Tunable High-Q Capacitors

One application presently under intense examination for possible miniaturization is that of the VCO used in the syn-

thesizer that generates the local oscillator signal. Currently, such VCO's are implemented using off-chip inductors (with Q's of at least 30) combined with off-chip voltage-tunable varactor diode capacitors (with Q's of at least 40). These relatively low Q values are justified for this VCO because in the synthesizer, this oscillator ends up slaved to a much more stable reference crystal oscillator, which cleans up the VCO's phase-noise spectrum at small f_m's through the action of a PLL. As such, the phase-noise specifications for this VCO are the easiest to satisfy in a given transceiver system, with numbers like −100 dBc/Hz at 10 kHz offset from the carrier (for European GSM) being typical.

Even with this seemingly easy goal, however, attempts at miniaturization based on conventional IC technologies fall well short of this mark. In particular, CMOS ring or relaxation oscillators attain only −60 dBc/Hz at 10 kHz offset [20]—not nearly adequate for GSM purposes. Furthermore, even slightly modified silicon CMOS and bipolar processes that include on-chip spiral inductors [21], or even bond wire inductors [22], yield LC VCO's with inadequate phase-noise performance (∼−85 dBc/Hz). A large part of the problem arises from the tunable capacitor implementation. Specifically, on-chip diodes used in place of previous off-chip varactor diodes exhibit excessive series resistance—much more than their off-chip varactor counterparts—and as a result, their Q's are severely lacking. In addition, the tuning range of such capacitors over available supply voltages is often limited to the point where trimming is required to set a starting capacitor value [23].

Recent demonstrations of voltage-tunable capacitors composed of micromachined, movable, metal plates now offer substantial improvements over on-chip diode-based capacitors. Fig. 4 presents the schematic of one such voltage-tunable micromachined capacitor [12], consisting of an aluminum top capacitor plate suspended by soft flexures above a bottom plate, in which the distance (and thus capacitance) between the plates is electrostatically varied by action of the underlying electrode. The prototype capacitor of Fig. 4 exhibited a tuning range of about 16% over a 5.5 V range of applied bias, with capacitance values on the order of 2.2 pF (achieved with four of these devices wired in parallel, each with $L_p = 200$ μm and $d = 1.5$ μm, nominally) and a Q of 62 at 1 GHz—all on par with off-chip varactor diodes [12].

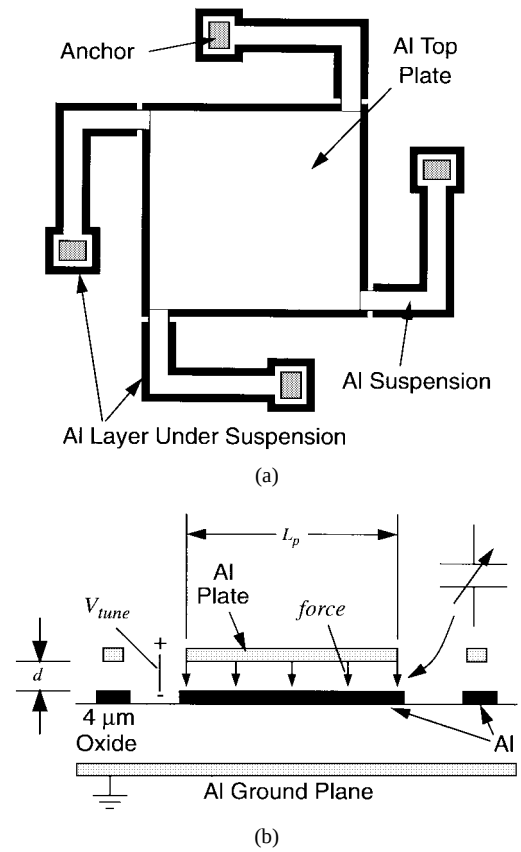

Fig. 4. (a) Overhead and (b) cross-sectional schematics of a voltage-tunable micromechanical capacitor [12].

B. Micromachined Inductors

Obviously, implementation of a miniature tunable capacitor solves only part of the problem. To achieve resonator tanks with adequate Q (at least for VCO's), high-Q inductors are required as well. As mentioned above, numerous attempts to implement spiral inductors using conventional IC technologies have so far yielded inductors with insufficient Q [1]–[3]. Even those using bond wires as inductors fall short on Q for many applications [22].

For the above reasons, research aimed at improving on-chip inductor performance via more exotic micromachining technologies is currently under way. Among the strategies utilized for this purpose are 1) the use of magnetic cores to enhance coupling in inductive coils and 2) removal of lossy substrates by fabricating inductors on suspended membranes, achieved via familiar back-side etching techniques. Fig. 5 presents two very recent applications of these methods. The inductor in Fig. 5(a) utilizes an NiFe core under a planar metal spiral to increase the achievable flux and attain 2.7 μH of inductance (for $W_{wind} = 50$ μm and $h_{wind} = 10$ μm, and ten turns in an area of 2×10 mm^2) with a Q of 6.6 at 4 MHz [13]. This configuration was found to give the highest Q relative to three other topologies combining metal coils with magnetic cores.

Fig. 5(b) presents the schematic of a miniature spiral inductor fabricated on a substrate-isolating platform (or membrane) and achieving an overall inductance of 115 nH with a Q of 22 at 275 MHz. Microwave/millimeter-wave inductors fabricated using similar techniques have achieved inductances on the order of 1.2 nH with associated self-resonance frequencies of 70 GHz with substrate removal, and 22 GHz without substrate removal, with expected Q's of 60–80 at 40 GHz. These inductors and others like them have achieved some of the highest Q values for on-chip inductors at their respective frequencies.

Despite the above promising results, the inductors of Fig. 5 are still inadequate for some applications within communication systems. In particular, as implied above, both designs, even the one with substrate removed, suffer from parasitic self-resonance problems that limit their frequency range. Self-resonance is generally not a problem when small

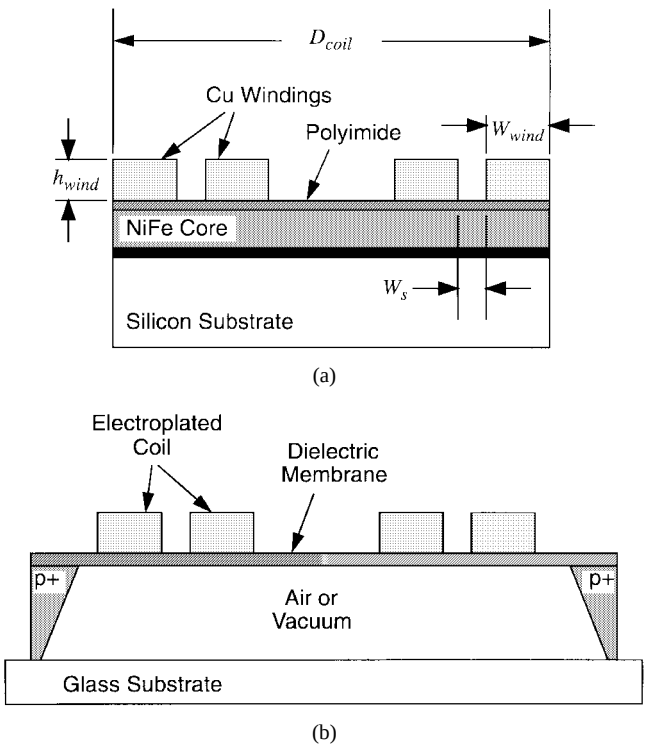

Fig. 5. Advanced integrated inductors utilizing micromachining processes. (a) Spiral inductor over an NiFe core. (b) Spiral inductor over an isolating platform [13], [14].

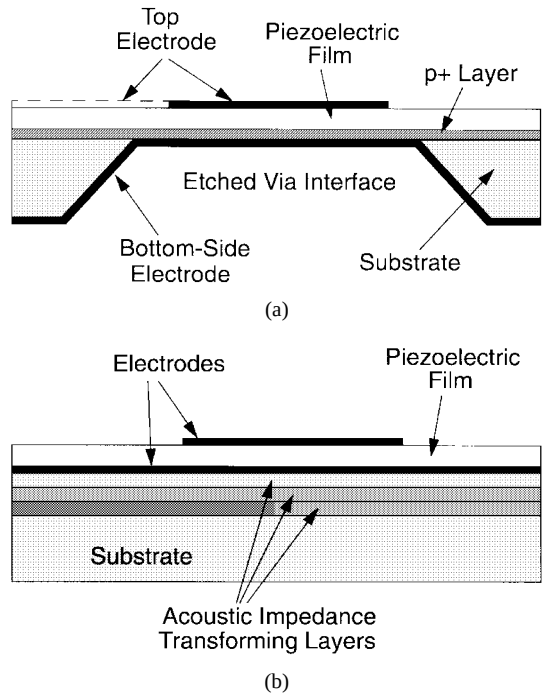

Fig. 6. Cross sections of two thin-film bulk-acoustic resonators. (a) A membrane supported FBAR resonator [4]. (b) A solidly mounted resonator [11].

inductance values are needed (e.g., <10 nH) but can be significant when requirements exceed 20 nH. Second, for the case of Fig. 5(a) and for others based upon its design, the magnetic core only reacts up to a certain frequency range, beyond which its permeability drops to an ineffective value [16]. Research to solve these problems is ongoing.

C. Thin-Film Bulk Acoustic Resonators

Assuming that Q's on the order of 40 can be achieved, the above tunable capacitors and on-chip inductors can potentially find use as resonator tanks for VCO's and low-Q RF filters, as well as elements for tunable couplers. However, given the present struggle to attain just these Q's, and with questions of susceptibility to microphonics and Brownian motion noise unanswered, it is unlikely that such elements could be utilized to replace the vibrating mechanical resonators (e.g., quartz crystals) used in the more demanding reference oscillator and channel-select filter functions. For these functions, as discussed in the context of Figs. 2 and 3, much higher Q's (in the thousands) are required.

With the knowledge that such Q's are already attainable using macroscopic vibrating mechanical tanks (e.g., quartz crystals, SAW's), much initial research had focused on developing exotic thin-film technologies to yield miniature versions of vibrating mechanical resonators operating under principles similar to their macroscopic counterparts. Fig. 6(a) presents the schematic of one such thin-film bulk-acoustic mode, piezoelectric resonator (FBAR), composed of deposited piezoelectric films sandwiched between conductors in a similar fashion to quartz crystals, all suspended on a thin membrane, and so acoustically isolated from the substrate. Such resonators constructed using aluminum nitride piezoelectric films have been demonstrated with Q's of over 1000 and resonance frequencies of 1.5–7.5 GHz [4], [5] in sizes of less than 400 $\times$ 400 μm^2. Although very promising, the device of Fig. 6(a) awaits improvements in process and trimming technologies. In addition, problems with the structural integrity of the supporting membrane have been reported [11].

One promising solution to the above drawbacks dispenses with the fragile membrane support and allows construction of the thin-film resonator directly over a solid substrate, as shown in Fig. 6(b). In this scheme, energy loss to the substrate (which would greatly attenuate the Q) is avoided by acoustically isolating the substrate from the piezoelectric resonator materials using impedance transformations obtained through strategic selection of the number and thickness of layers separating the two media [11]. Although the implementation of such a solidly mounted resonator (SMR) requires more careful deposition of layers, it promises to greatly improve the resiliency of thin-film bulk-acoustic resonators.

As with other novel technologies discussed here, thin-film bulk-acoustic resonators, with all of their advantages, still have several important drawbacks that presently hinder their use. First, a convenient and effective means for trimming and tuning these resonators is not yet available. Such a trimming technology is vitally important, especially if groups of these resonators are to be used to implement small percent bandwidth filters with small shape factors. Second, these filters are presently most appropriate for the

high UHF- and S-band frequency ranges, becoming overly thick and cumbersome at lower frequencies.

D. Micromechanical Resonators and Filters

For lower frequency applications, planar IC-compatible micromachining processes have now realized flexural-mode micromechanical resonators in a variety of structural materials, and (so far) in a range of frequencies from low frequency (LF) to very high frequency (VHF). Q's exceeding 80 000 in vacuum have been measured for LF flexural-mode resonators constructed in surface-micromachined polysilicon [24], while Q's on the order of 20 000 have been achieved at 70 MHz (VHF) in single-crystal silicon material [25]. Since the use of this technology for high-frequency applications is quite recent, its ultimate frequency limit is as yet unknown. Operating frequencies into the gigahertz range, however, are not unreasonable [9], [10].

In addition to their enormous Q values and wide applicable frequency range, micromechanical resonators are extremely flexible from a design perspective, having several features that greatly simplify the design and implementation of complex resonator systems. Among their most attractive features are:

1) an inherent voltage-controlled frequency tunability [26] and switchability [10];
2) an amenability to trimming [27];
3) wide flexibility in available geometries (leading to a seemingly limitless range of possible designs);
4) flexibility in the choice of structural materials used;
5) flexibility in the type of transduction used (electrostatic, piezoelectric, and magnetostrictive have all been utilized in the past).

On top of all of this, successful construction of devices using such resonators is relatively straightforward, since critical features are usually defined by a single masking step, which itself is part of a planar process largely compatible with conventional IC processes.

The above features, in particular those associated with tuning and design flexibility, have greatly accelerated the rate at which more complex oscillator and filtering applications of the technology have been realized. Specifically, micromechanical filters comprised of multiple resonators coupled by soft mechanical springs have recently been implemented with performance attributes comparable to some of the best high-Q filters available. Fig. 7(a) presents the perspective-view schematic for an HF-range, two-resonator filter, composed of two identical clamped-clamped beam micromechanical resonators coupled by a flexural-mode coupling beam. As shown, resonance motion perpendicular to the substrate is excited and sensed electrostatically using a combination of dc-bias V_P and ac voltages v_i applied between the conductive resonators and electrodes underlying each resonator. In this device, the coupling beams couple energy between resonators, creating a coupled two-resonator system with two modes of vibration that define

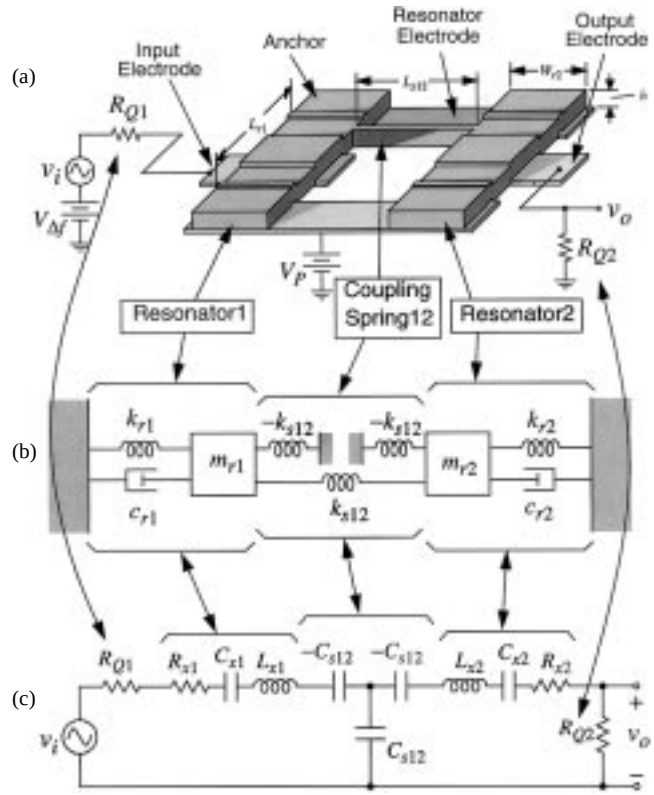

Fig. 7. (a) Perspective-view schematic of an HF micromechanical filter in a typical bias and excitation configuration. (b) Equivalent mechanical circuit for the filter of (a) using quarter-wavelength coupling. (c) Equivalent electrical circuit for the filter of (a), again with quarter-wavelength coupling.

the passband of the filter. The center frequency of the filter f_o is determined primarily by the resonance frequency of the identical resonators, while its bandwidth is dictated by the relative stiffnesses of the coupling beam and resonators and is given specifically by the expression

$$\mathrm{BW} = \left(\frac{f_o}{k_{ij}}\right)\left(\frac{k_{sij}}{k_r}\right) \tag{2}$$

where k_{sij} is the stiffness of the coupling beam joining resonators i and j, k_r is the resonator stiffness, and k_{ij} is a normalized coupling coefficient found in filter cookbooks [28]. By using electromechanical analogies, equivalent electrical circuits resembling LC ladders can be derived for micromechanical filters, as illustrated in Fig. 7(b) and (c). Such circuit modeling strategies make micromechanical filters amenable to computer-aided design, synthesis, and verification and allow the use of the already enormous existing knowledge on LC ladder filter synthesis for micromechanical filter design.

To date, two-resonator micromechanical bandpass filters (Fig. 8) have been demonstrated with frequencies up to 14.5 MHz, percent bandwidths on the order of 0.2%, and insertion losses less than 1 dB [29]. Higher order, three-resonator filters with frequencies near 455 kHz have also been achieved (Fig. 9), with equally impressive insertion losses for 0.09% bandwidths and with more than 64 dB of passband rejection [30], [31]. The filter of Fig. 9 features

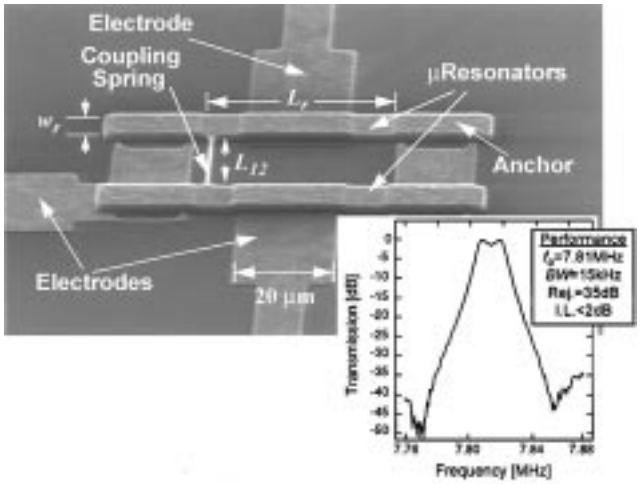

Fig. 8. SEM of a two-resonator, surface-micromachined, HF micromechanical filter with a measured frequency characteristic [29].

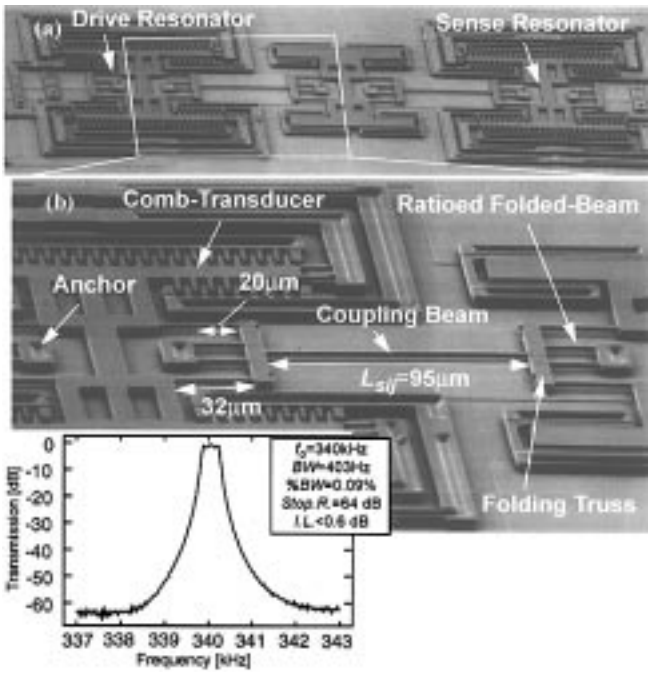

Fig. 9. SEM's of a surface-micromachined, medium-frequency, three-resonator micromechanical filter with a measured transmission spectrum [31].

balanced comb-transduction for feedthrough suppression, low velocity coupling, and frequency tuning electrodes, adeptly illustrating the complexity and flexibility achievable using this technology.

In addition to filters, LF high-Q oscillators, fully integrated with sustaining CMOS electronics, have also already been demonstrated in this technology. Fig. 10 presents the overhead-view scanning electron microscope (SEM) of a 16.5 kHz prototype of such an oscillator [32]. Recent studies of similar fully integrated oscillators have shown phase-noise performance expected of high-Q oscillator operation, but they also show additional sources of phase noise related to nonlinear amplitude perturbations caused by $1/f$

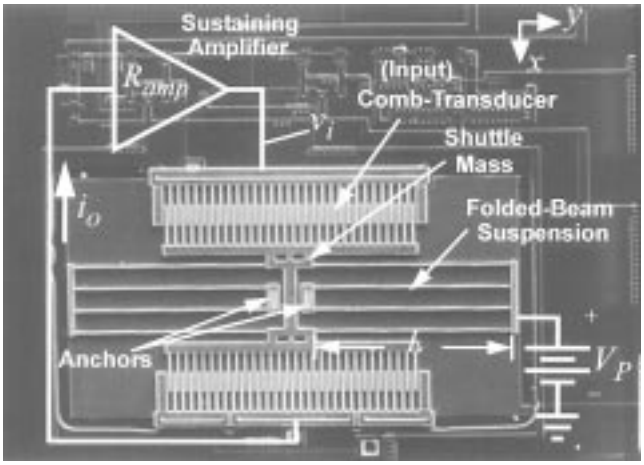

Fig. 10. SEM of a 16.5 kHz CMOS microresonator oscillator with schematics explicitly depicting circuit topology. The microresonator occupies $420 \times 230\ \mu\text{m}^2$ [32].

noise [33]. Thus, much work is still needed to attain optimal performance of micromechanical resonator oscillators. Research is also currently under way to extend the frequency of this oscillator to the popular 10 MHz frequency of reference oscillators used in many transceivers, and to do so in a fashion that reduces the overall temperature coefficient of the oscillator.

Again, as with the other technologies, micromechanical resonator devices are not without their drawbacks. Among the more disturbing of them are the need for vacuum to attain high Q, an unaided temperature coefficient of -10 ppm/°C [10] (not as good as quartz), and uncertainties concerning ultimate dynamic range and power-handling capability [10]. Research on micromechanical resonators and their applications is ongoing.

E. Micromachined Filters for K-Band and Higher

For transceivers operating at K-band and higher, preselect or image-reject filters with bandwidths of 1–8% are implemented using microwave and millimeter-wave components. Low loss is essential for such front-end filters, since they are placed just after the antenna, before any amplification, and thus, their loss adds directly to the noise figure of the receiver and reduces the effective radiated power from the transmitter. Again, high-Q resonators are required to minimize this loss, and again, this can only be achieved using external elements such as dielectric resonators or waveguide components, which increase the size and cost of the receiver.

To address this problem, filter implementation using monolithic transmission-line (T-line) resonator approaches has been investigated. The main problem with using T-line resonators on Si or GaAs involves the underlying high dielectric constant substrate (with $\varepsilon_r = 12$–13). It is well known that T-lines integrated on these substrates suffer from radiation loss into the dielectric and increased ohmic loss due to their small dimensions. This has limited the Q of planar resonators on Si/GaAs to 40–60 at 30–60 GHz, which is not acceptable for low-loss filters. An

intermediate solution is to integrate the planar filters on teflon or quartz substrates with $\varepsilon_r = 2.2$–4, This results in a resonator Q of 200–300 at 30–60 GHz, but is not compatible with Si/GaAs integrated circuits and therefore requires transitions between millimeter-wave active circuits and the external filters.

One way to dramatically increase the Q of a planar resonator on Si/GaAs is to integrate the resonator on a thin dielectric membrane (1–1.5 μm thick) and to enclose the resonator in a microshielded cavity 100–500 μm high [34]–[40]. The fabrication sequence required for such a resonator utilizes standard micromachining processes and includes 1) the deposition of a silicon nitride membrane; 2) back etching of the wafer; 3) etching and filling of via-holes with gold; and 4) attachment of several wafers together to form a miniature stack. The T-line resonators are effectively suspended in free space and are therefore limited only by ohmic loss. Furthermore, the resonators are wider than their counterparts on Si/GaAs (so as to obtain the same filter impedance), which considerably reduces their ohmic loss. Recently measured Q's of quarter-wavelength resonators ($W = 700$ μm, $h = 200$ μm) at 60 GHz are around 600, which is ten times better than comparable resonators on Si/GaAs and only three to four times worse than waveguide resonators [36].

Micromachined T-lines on thin dielectric membranes have been used extensively in filter designs from 14 to 250 GHz [34]–[39]. The filters follow standard designs (elliptic, Chebyshev, etc.), use well-known transmission-line types (coplanar waveguide lines, stripline, suspended microstrip lines, etc.), and result in excellent performance. A lot of attention has been placed on the transition between the Si/GaAs substrate and the membrane T-lines, and a transition with better than -20 dB return loss is attainable up to 60 GHz [35], [36]. Recent results obtained for a four-pole elliptic filter at 60 GHz show an insertion loss of only 1.5 dB and a rejection better than -40 dB (Fig. 11) [36]. This filter is state of the art and is only 0.5–0.7 dB more lossy than its waveguide implementation (but with a 1000$\times$ size reduction).

Another application of micromachining is the fabrication of three-dimensional cavities to synthesize miniature waveguide components at 10–60 GHz. In this case, a reduced height resonant waveguide cavity (with dimensions of $\lambda/2$-square) is etched in a silicon wafer and fed either by a slot transition or by bond wires. Since the fields are not confined to planar resonators, these structures have yielded Q's around 500 at 10 GHz, and up to 1100 at 30 GHz [41], [42]. Research is under way to use these miniature waveguide cavities in satellite filters and low-phase noise oscillators.

One final advantage of micromachined lines is the micropackaging aspect of this technique. As seen in Fig. 11, the filter (or any component inside the microcavity) is completely shielded and therefore will not couple any RF energy to the outside world. The typical measured isolation between adjacent transmission lines is -50 dB at 30 GHz, and -45 dB between closely spaced filter banks at 10 GHz [43], [44]. Such micropackaging techniques are expected

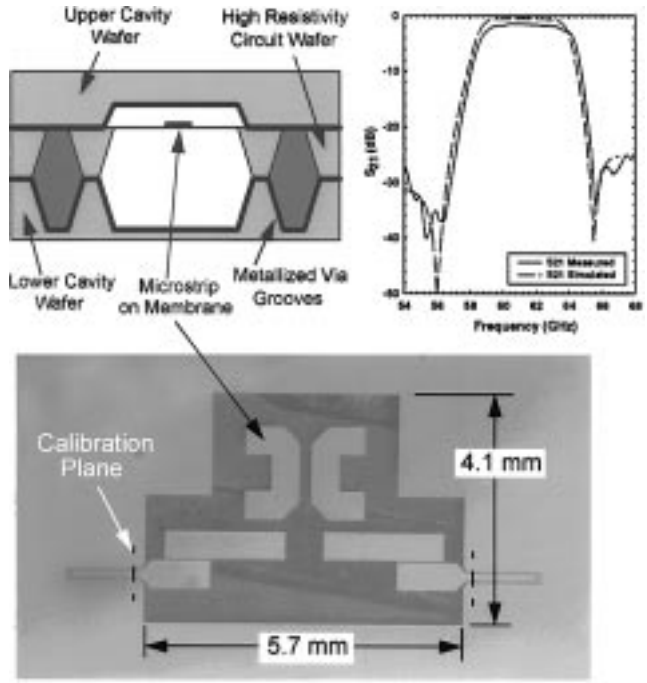

Fig. 11. A 60 GHz, 8% bandwidth, four-pole micromachined elliptic filter with a resonator width of 500 μm and a resonator Q of 500. The insertion loss in the passband is 1.5 dB referenced to the calibration planes.

eventually to allow the integration of the millimeter-wave transmitters and receivers on the same chip. Research toward this goal is ongoing.

F. Micromechanical Switches

In addition to the filter and oscillator research described above, a good amount of research effort has focused on the implementation of micromechanical switches for antenna or filter-path selection in multiband communications systems, and for deployment of phased-array antennas in higher frequency systems operating past Ka-band (where antennas become small enough for arrays). Such switches are often characterized by metrics describing switching speed and off/on impedance. So far, the majority of switches for communications have operated via electrostatic actuation.

Fig. 12 presents the cross-sectional schematic of a typical single-pole, single-throw micromechanical switch. Such switches are now developed by several U.S. industries [45]–[50]. As shown, the switch of Fig. 12 utilizes an air-bridge design, in which a bridge of conducting material is suspended 3–4 μm over a coplanar line. The top and bottom plates of this switch are constructed of evaporated or plated aluminum or gold. For the case of microwave/millimeter-wave switches, actual metal-to-metal contact is not necessary; rather, a step change in plate-to-plate capacitance also realizes switching. Thus, in high-frequency applications, a protective nitride film (on the order of 1000 Å) often resides above the bottom electrode plate to prevent sticking when plates are pulled together. The dimensions of the top plate are around 300–400 μm-square for a 10–20 GHz switch, and 200 μm for 60 GHz designs.

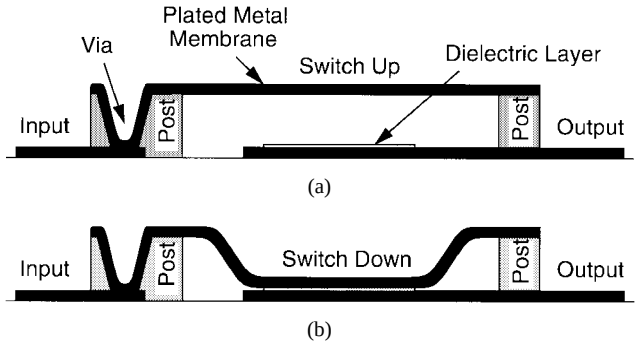

Fig. 12. Cross-sectional schematics of a typical micromechanical switch. (a) Switch up. (b) Switch down [45].

Micromechanical switches have been fabricated in both series and shunt (to ground) configurations. The insertion loss of a typical shunt switch in the "on-state" position (bridge is up and capacitance is low) is around 0.1 dB at 10 GHz and increases linearly with frequency to 0.6 dB at 60 GHz. The isolation of a micromechanical switch in the "off-state" position (bridge is low and capacitance is high) is directly proportional to the bridge area and can be designed to be −20 to −25 dB at 20 GHz, at 40 GHz, or at 60 GHz [45]. To date, metal-to-metal series switches that have shown impressive "off-state" (bridge is up and capacitance is low) isolation at 1–4 GHz (−60 to −50 dB), with a very low "on-state" (bridge is down and metal-to-metal contact is achieved) insertion loss (−0.1 dB), have been demonstrated [46]. Currently, most shunt switches can safely handle 0.5–2 W of RF power in the "on-state" position before hot-switching becomes a problem, a phenomena where the RF voltage under the switch in the "on-state" position develops enough of a voltage to actually pull the micromechanical bridge down.

Micromechanical switches, such as those shown in Fig. 12, normally outperform those implemented with PIN diodes or GaAs field-effect transistors (FET's) in "on-state" insertion loss and "off-state" isolation. They also consume zero power when activated, unlike their solid-state counterparts, which sink a finite amount of current when activated. However, most are much slower than PIN or FET diode switches (4–20 μs versus 1–40 ns), and they so far require relatively high actuation voltages (20–60 V versus 3–5 V). Micromechanical switches are also prone to stiction problems in a metal-to-metal switch and dielectric charging problems in case of a nitride film between the electrodes, and research is still being conducted to evaluate their ultimate lifetimes (now at billions of cycles). However, there is one aspect of micromechanical switches that makes them extremely favorable for communications systems: Micromechanical switches are extremely linear devices. A 2 GHz switch in a two-tone experiment resulted in unmeasured intermodulation products and an extrapolated IP3 of 66 dBm (4000 W).

Micromechanical switches are particularly attractive in low-power RF/microwave/millimeter-wave communications systems because of their low distortion characteristics, and for active antenna applications (phased arrays, power combining, etc.) because of their very low insertion loss (which eliminates the need for loss-recovering power amplifiers) and near-zero dc power consumption (which allows substantial power savings). Research on micromechanical switches continues, and new versions with all of the above advantages, but with much smaller actuation voltage requirements and much faster response times, are presently under investigation [50].

G. Micromachined Antennas and Synthesized Substrates

Micromachining technologies first found use for antennas at millimeter-wave and terahertz frequencies to alleviate loss and size constraints at such high frequencies. In particular, antennas on Si/GaAs and even quartz dielectrics are inefficient radiators at millimeter-wave and terahertz frequencies due to the electrical thickness of the underlying substrate. Micromachining has therefore been used to suspend dipole or slot radiators on thin dielectric membranes (without the shielding cavities described in previous filters), with the planar antennas then effectively radiating in free space. Anisotropic etching has also been used to integrate silicon pyramidal cavities that act as miniature integrated horns around the dipole antennas, directing the radiated energy very efficiently in the forward direction [51], [52].

For microwave frequencies, membrane technology with $\varepsilon_r \sim 1$ results in physically large antennas and thus is not practical. Therefore, at these frequencies, membrane approaches are avoided, and micromachining is instead used to synthesize artificial dielectric-constant substrate materials underneath the antennas. In particular, by etching a portion of the dielectric or by strategically choosing the density of via-holes underneath an antenna, a dielectric constant between one (complete removal) and ε_r (no removal) can be synthesized [Fig. 13(a)]. Using such techniques, the efficiency of microstrip antennas at 12–13 GHz has been increased from 55% ($\varepsilon_r = 10$) to 85% ($\varepsilon_{synth} = 2.3$) [53], [54]. Similar techniques have also been applied at 77 GHz for automotive radar applications [55]. Furthermore, the dielectric constant around a planar antenna can be artificially tailored so as to further increase radiation efficiency and bandwidth.

Last, micromachining techniques have been used to synthesize photonic bandgap materials on high-resistivity silicon substrates at 30 GHz by etching a periodic pattern of hexagonal holes ($d = 1050$ μm, period $= 1700$ μm) in the silicon substrate [Fig. 13(b)] [56], [57]. The holes create an "exclusion" of electromagnetic modes in the dielectric substrate and therefore dramatically increase the radiation efficiency of planar antennas (from 30% without holes to 85% with holes). It is expected that photonic bandgap materials will play an important role in the integration of high-efficiency antennas on Si and GaAs substrates.

IV. Conclusions

Due to the need for Q values beyond the capabilities of conventional IC technologies, board-level passive components continue to occupy a substantial portion of the

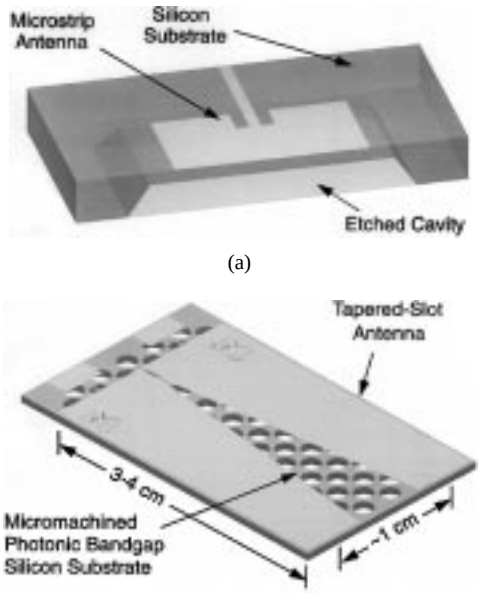

Fig. 13. (a) Microstrip antennas on synthesized dielectrics built using partial removal of the silicon substrate. (b) A high-efficiency tapered slot antenna on a micromachined photonic bandgap substrate at 30 GHz.

overall area in superheterodyne transceivers, presenting a key bottleneck against further miniaturization. Although there have been many research efforts aimed at replacing superheterodyne architectures with alternatives that use higher levels of transistor integration to eliminate the need for off-chip passive elements, none of these new approaches has yet been able to match, let alone improve, the performance of existing systems.

Micromechanical resonators and micromachined passives, on the other hand, offer an alternative set of strategies for transceiver miniaturization and improvement, the simplest of which may merely retain proven superheterodyne architectures, the boldest of which may revolutionize the way future transceivers are designed. In particular, the availability of high-Q micromachined filters, with their tiny size and zero dc power dissipation, may encourage future architectures that take advantage of large arrays of such filters to yield novel transceivers with multiband capability and enhanced security against jamming or interception. In combination with low clock-rate subsampling downconverters [8], such an array architecture might also provide substantial power savings over previous systems, especially when used in frequency-hopping scenarios. Needless to say, research on micromachined devices for communications continues on both device and system levels, with promises to influence wireless communications greatly in the near future.

ACKNOWLEDGMENT

The authors gratefully acknowledge substantial contributions from former and present graduate students, in particular F. Bannon III, K. Wang, and J. Clark, who are largely responsible for the micromechanical filter results, and C.-Y. Chi, T. Weller, S. Robinson, A. Brown, R. Henderson, and S. Pacheco, who are responsible for the microwave and millimeter-wave effort.

REFERENCES

[1] E. Frian, S. Meszaros, M. Chuaci, and J. Wight, "Computer-aided design of square spiral transformers and inductors," in *1989 IEEE MTT-S Dig.*, pp. 661–664.
[2] N. M. Nguyen and R. G. Meyer, "Si IC-compatible inductors and LC passive filters," *IEEE J. Solid-State Circuits*, vol. 25, pp. 1028–1031, Aug. 1990.
[3] ——, "A 1.8-GHz monolithic LC voltage-controlled oscillator," *IEEE J. Solid- State Circuits*, vol. 27, no. 3, pp. 444–450, 1992.
[4] S. V. Krishnaswamy, J. Rosenbaum, S. Horwitz, C. Yale, and R. A. Moore, "Compact FBAR filters offer low-loss performance," *Microwaves RF*, pp. 127–136, Sept. 1991.
[5] R. Ruby and P. Merchant, "Micromachined thin film bulk acoustic resonators," in *Proc. 1994 IEEE Int. Frequency Control Symp.*, Boston, MA, June 1–3, 1994, pp. 135–138.
[6] P. R. Gray and R. G. Meyer, "Future directions in silicon IC's for RF personal communications," in *Proc., 1995 IEEE Custom Integrated Circuits Conf.*, Santa Clara, CA, May 1–4, 1995, pp. 83–90.
[7] A. A. Abidi, "Direct-conversion radio transceivers for digital communications," *IEEE J. Solid-State Circuits*, vol. 30, pp. 1399–1410, Dec. 1995.
[8] D. H. Shen, C.-M. Hwang, B. B. Lusignan, and B. A. Wooley, "A 900-MHz RF front-end with integrated discrete-time filtering," *IEEE J. Solid-State Circuits*, vol. 31, pp. 1945–1954, Dec. 1996.
[9] C. T.-C. Nguyen, "High-Q micromechanical oscillators and filters for communications," in *Proc. 1997 IEEE Int. Symp. Circuits and Systems*, Hong Kong, June 9–12, 1997, pp. 2825–2828.
[10] ——, "Frequency-selective MEMS for miniaturized communication devices," in *Proc. 1998 IEEE Aerospace Conf.*, Snowmass, CO, Mar. 21–28, 1998, pp. 445–460.
[11] K. M. Lakin, G. R. Kline, and K. T. McCarron, "Development of miniature filters for wireless applications," *IEEE Trans. Microwave Theory Tech.*, vol. 43, pp. 2933–2939, Dec. 1995.
[12] D. J. Young and B. E. Boser, "A micromachined variable capacitor for monolithic low-noise VCO's," in *Tech. Dig. 1996 Solid-State Sensor and Actuator Workshop*, Hilton Head Island, SC, June 3–6, 1996, pp. 86–89.
[13] J. A. Von Arx and K. Najafi, "On-chip coils with integrated cores for remote inductive powering of integrated microsystems," in *Dig. Tech. Papers 1997 Int. Conf. Solid-State Sensors and Actuators (Transducers'97)*, Chicago, IL, June 16–19, 1997, pp. 999–1002.
[14] B. Ziaie, N. K. Kocaman, and K. Najafi, "A generic micromachined silicon platform for low-power, low-low miniature transceivers," in *Dig. Tech. Papers 1997 Int. Conf. Solid-State Sensors and Actuators (Transducers'97)*, Chicago, IL, June 16–19, 1997, pp. 257–260.
[15] M. G. Allen, "Micromachined intermediate and high frequency inductors," in *Proc. 1997 IEEE Int. Symp. Circuits and Systems*, Hong Kong, June 9–12, 1997, pp. 2829–2832.
[16] C. H. Ahn, Y. J. Kim, and M. G. Allen, "A fully integrated micromachined toroidal inductor with nickel-iron magnetic core (the switched DC/DC boost converter application)," in *Dig. Tech. Papers 7th Int. Conf. Solid-State Sensors and Actuators (Transducers'93)*, Yokohama, Japan, June 7–10, 1993, pp. 70–73.
[17] J. D. Cressler, D. L. Harame, H. H. Comfort, J. M. C. Stork, B. S. Meyerson, and T. E. Tice, "Silicon–germanium heterojunction bipolar technology: The next leap for silicon?" in *Dig. Tech. Papers 1994 ISSCC*, San Francisco, CA, Feb. 1994, pp. 24–27.
[18] W. P. Robins, *Phase Noise in Signal Sources*. London, UK: Peregrinus, 1982.
[19] N. Slawsby, "Frequency control requirements of radar," in *Proc. 1994 IEEE Int. Frequency Control Symp.*, June 1–3, 1994, pp. 633–640.

[20] T. C. Weigandt, B. Kim, and P. R. Gray, "Analysis of timing jitter in CMOS ring oscillators," in *Proc. ISCAS'94*, June 1994, pp. 27–30.
[21] N. M. Nguyen, "A 1.8-GHz monolithic LC voltage-controlled oscillator," *IEEE J. Solid-State Circuits*, vol. 27, pp. 444–450, Mar. 1992.
[22] J. Craninckx and M. S. J. Steyaert, "A 1.8 GHz CMOS low-phase-noise voltage controlled oscillator with prescaler," *IEEE J. Solid-State Circuits*, vol. 30, pp. 1474–1482, Dec. 1995.
[23] M. Soyuer, K. A. Jenkins, J. N. Burghartz, and M. D. Hulvey, "A 3V 4GHz NMOS voltage-controlled oscillator with integrated resonator," in *Tech. Dig. 1996 ISSCC*, San Francisco, CA, Feb. 1996, pp. 394–395.
[24] C. T.-C. Nguyen and R. T. Howe, "Quality factor control for micromechanical resonators," in *Tech. Dig. IEEE Int. Electron Devices Meeting*, San Francisco, CA, Dec. 14–16, 1992, pp. 505–508.
[25] A. N. Cleland and M. L. Roukes, "Fabrication of high frequency nanometer scale mechanical resonators from bulk Si crystals," *Appl. Phys. Lett.*, vol. 69, no. 18, pp. 2653–2655, Oct. 28, 1996.
[26] R. T. Howe and R. S. Muller, "Resonant microbridge vapor sensor," *IEEE Trans. Electron Devices*, vol. ED-33, pp. 499–506, 1986.
[27] K. Wang, A.-C. Wong, W.-T. Hsu, and C. T.-C. Nguyen, "Frequency-trimming and Q-factor enhancement of micromechanical resonators via localized filament annealing," in *Dig. Tech. Papers 1997 Int. Conf. Solid-State Sensors and Actuators*, Chicago, IL, June 16–19, 1997, pp. 109–112.
[28] A. I. Zverev, *Handbook of Filter Synthesis.* New York: Wiley, 1967.
[29] F. D. Bannon III and C. T.-C. Nguyen, "High frequency microelectromechanical IF filters," in *Tech. Dig. 1996 IEEE Electron Devices Meeting*, San Francisco, CA, Dec. 8–11, 1996, pp. 773–776.
[30] K. Wang and C. T.-C. Nguyen, "High-order micromechanical electronic filters," in *Proc. 1997 IEEE Int. Micro Electro Mechanical Systems Workshop*, Nagoya, Japan, Jan. 26–30, 1997, pp. 25–30.
[31] K. Wang, J. R. Clark, and C. T.-C. Nguyen, "Q-enhancement of micromechanical filters via low-velocity spring coupling," in *Proc. 1997 IEEE Int. Ultrasonics Symp.*, Toronto, Ont., Canada, Oct. 5–8, 1997, to be published.
[32] C. T.-C. Nguyen and R. T. Howe, "CMOS micromechanical resonator oscillator," in *Tech. Dig. IEEE Int. Electron Devices Meeting*, Washington, DC, Dec. 5–8, 1993, pp. 199–202.
[33] T. Roessig, R. T. Howe, and A. P. Pisano, "Nonlinear mixing in surface-micromachined tuning fork oscillators," in *Proc. 1997 IEEE Frequency Control Symp.*, Orlando, FL, May 27–28, 1997, to be published.
[34] C. Y. Chi and G. M. Rebeiz, "Planar microwave and millimeter-wave lumped elements and coupled-line filters using micromachining techniques," *IEEE Trans. Microwave Theory Tech.*, vol. 43, pp. 730–738, Apr. 1995.
[35] T. M. Weller, L. P. Katehi, and G. M. Rebeiz, "High performance microshield line components," *IEEE Trans. Microwave Theory Tech.*, vol. 43, pp. 534–543, Mar. 1995.
[36] P. Blondy, A. R. Brown, D. Cros, and G. M. Rebeiz, "Low-loss micromachined elliptic filters for millimeter wave telecommunication systems," presented at the IEEE International MTT-S Symposium, June 1998.
[37] G. M. Rebeiz, L. P. Katehi, T. M. Weller, C. Y. Chi, and S. V. Robertson, "Micromachined filters for microwave and millimeter-wave applications," *Int. J. Microwave Millimeter-Wave Computer Aided Eng.*, vol. 7, pp. 149–166, Feb. 1997.
[38] S. V. Robertson, L. P. Katehi, and G. M. Rebeiz, "Micromachined W-band filters," *IEEE Trans. Microwave Theory Tech.*, vol. 44, pp. 598–606, Apr. 1996.
[39] C. Y. Chi and G. M. Rebeiz, "Conductor-loss limited stripline resonators and filters," *IEEE Trans. Microwave Theory Tech.*, vol. 44, pp. 626–630, Apr. 1996.
[40] T. M. Weller, L. P. Katehi, and G. M. Rebeiz, "A 250 GHz microshield band-pass filter," *IEEE Microwave Guided Wave Lett.*, vol. 5, pp. 153–155, May 1995.
[41] J. Papapolymerou, J. C. Cheng, J. East, and L. Katehi, "A micromachined high-Q X-band resonator," *IEEE Microwave Guided Wave Lett.*, vol. 7, pp. 168–170, June 1997.
[42] A. R. Brown, P. Blondy, K. Hong, and G. M. Rebeiz, "Low-loss millimeter-wave filters and high-Q micromachined cavity resonators," U.S. Army Research Office Interim Rep., Dec. 18, 1997.
[43] R. F. Drayton, R. M. Henderson, and L. P. B. Katehi, "Advanced monolithic packaging concepts for high performance circuits and antennas," in *Dig. 1996 IEEE MTT-S*, June 1996, pp. 1615–1618.
[44] A. R. Brown and G. M. Rebeiz, "Micromachined micropackaged filter banks," *IEEE Microwave Guided Wave Lett.*, vol. 8, pp. 158–160, Mar. 1998.
[45] C. Goldsmith, J. Randall, S. Eshelman, T. H. Lin, D. Denniston, S. Chen, and B. Norvell, "Characteristics of micromachined switches at microwave frequencies," in *Dig. IEEE MTT-S*, June 1996, pp. 1141–1144.
[46] J. Yao and M. F. Chang, "A surface micromachined miniature switch for telecommunications applications with signal frequencies from DC to 4 GHz," in *Proc. 8th Int. Conf. Solid-State Sensors and Actuators, Transducers*, June 1995, pp. 384–387.
[47] Personal communications, Northrop Grumman, Baltimore, MD, 1997.
[48] Personal communications, HRL Laboratories, Malibu, CA, 1997.
[49] Personal communications, Honeywell Technology Center, Minneapolis, MN, 1997.
[50] S. Pacheco, C. T.-C. Nguyen, and L. P. B. Katehi, "Micromechanical electrostatic K-band switches," presented at the IEEE MTT-S International Microwave Symposium, June 1998.
[51] G. M. Rebeiz, D. P. Kasilingam, Y. Guo, P. A. Stimpson, and D. B. Rutledge, "Monolithic millimeter-wave two-dimensional horn imaging arrays," *IEEE Trans. Antennas Propagat.*, vol. 38, pp. 1473–1482, Sept. 1990.
[52] W. Y. Ali-Ahmad and G. M. Rebeiz, "An 86–106 GHz quasi-integrated low-noise receiver," *IEEE Trans. Microwave Theory Tech.*, vol. MTT-41, pp. 558–564, Apr. 1993.
[53] G. P. Gauthier, A. Courtay, and G. M. Rebeiz, "Microstrip antennas on synthesized low dielectric constant substrates," *IEEE Trans. Antennas Propagat.*, vol. AP-45, pp. 1310–1314, Aug. 1997.
[54] J. Papapolymerou, R. F. Drayton, and L. Katehi, "Micromachined patch antennas," *IEEE Trans. on Antennas Propagat.*, vol. AP-46, pp. 275–283, Feb. 1998.
[55] M. Stotz, G. Gottwald, and H. Haspeklo, "Planar millimeter-wave antennas using SiNx-membranes on GaAs," *IEEE Trans. Microwave Theory Tech.*, vol. 44, pp. 1593–1595, Sept. 1996.
[56] T. J. Ellis and G. M. Rebeiz, "MM-wave tapered slot antennas on micromachined photonic bandgap dielectrics," in *Proc. IEEE MTT-S Int. Microwave Symp.*, June 1996, pp. 1157–1160.
[57] T. J. Ellis, J. Muldavin, and G. M. Rebeiz, submitted for publication.

Clark T.-C. Nguyen (Member, IEEE) was born in Austin, TX, on March 29, 1967. He received the B.S., M.S., and Ph.D. degrees from the University of California at Berkeley in 1989, 1991, and 1994, respectively, all in electrical engineering and computer sciences.

In 1995, he joined the Faculty of the University of Michigan, Ann Arbor, where he currently is an Assistant Professor in the Department of Electrical Engineering and Computer Science. From 1995 to 1997, he was a Member of the National Aeronautics and Space Administration (NASA)'s New Millennium Integrated Product Development Team on Communications, which roadmaps future communications technologies for NASA use into the turn of the century. He now is a Consulting Member. His research interests focus upon microelectromechanical systems and include integrated micromechanical signal processors and sensors, merged circuit/micromechanical technologies, radio-frequency communication architectures, and integrated circuit design and technology.

Prof. Nguyen received the 1938E Award for Research and Teaching Excellence from the University of Michigan in 1988 and is a Finalist for the 1998 *Discover* magazine Technological Innovation Awards.

Linda P. B. Katehi (Fellow, IEEE) received the B.S.E.E. degree from the National Technical University of Athens, Greece, in 1977, and the M.S.E.E. and Ph.D. degrees from the University of California, Los Angeles, in 1981 and 1984, respectively.

In 1984, she joined the Faculty of the Department of Electrical Engineering and Computer Science of the University of Michigan, Ann Arbor. Since then, she has been interested in the development and characterization (theoretical and experimental) of microwave, millimeter printed circuits, the computer-aided design of very-large-scale-integration interconnects, the development and characterization of micromachined circuits for millimeter-wave and submillimeter-wave applications, and the development of low-loss lines for terahertz-frequency applications. She also has been studying theoretically and experimentally various types of uniplanar radiating structures for hybrid-monolithic and monolithic oscillator and mixer designs.

Dr. Katehi received the IEEE AP-S W. P. King (Best Paper Award for a Young Engineer) in 1984, the IEEE AP-S S. A. Schelkunoff Award (Best Paper Award) in 1985, the NSF Presidential Young Investigator Award and an URSI Young Scientist Fellowship in 1987, the Humboldt Research Award and the University of Michigan Faculty Recognition Award in 1994, the IEEE MTT-S Microwave Prize in 1996, and the Best Paper Award from the International Society on Microelectronics and Advanced Packaging. She is a member of the IEEE Antennas and Propagation and Microwave Theory and Techniques societies, Sigma XI, Hybrid Microelectronics, and URSI Commission D. She was a member of AP-S ADCOM from 1992 to 1995. She is an Associate Editor for IEEE TRANSACTIONS ON MICROWAVE THEORY AND TECHNIQUES.

Gabriel M. Rebeiz (Fellow, IEEE) received the Ph.D. degree in electrical engineering from the California Institute of Technology, Pasadena, in 1988.

He joined the Faculty of the University of Michigan, Ann Arbor, in 1988 and became Associate Professor in 1992. He was a Visiting Professor at Chalmers University of Technology, Göteborg, Sweden, in 1992 and a Visiting Professor at the Ecole Normale Superieur, France, in 1993. In 1997, he was a Visiting Professor at Tohoku University, Sendai, Japan. His interests are in applying micromachining techniques in silicon and GaAs for the development of low-loss and low-cost microwave antennas, components and subsystems for wireless applications, and satellite communication systems. He also is interested in the development of planar collision-avoidance sensors for automotive applications and in millimeter-wave imaging arrays, monopulse tracking systems, and phased arrays. He is the author of 70 papers published in refereed journals and more than 120 papers presented at national and international conferences.

Prof. Rebeiz received the National Science Foundation Presidential Young Investigator Award in April 1991 and the URSI International Isaac Koga Gold Medal Award for Outstanding International Research in August 1993. He received the Research Excellence Award in April 1995 from the University of Michigan. Together with his students, he received Best Paper Awards at JINA 1990, IEEE-MTT 1992 and 1994–1997, and IEEE-AP 1992 and 1995.